

# Computational Multispectral Flash

Henryk Blasinski and Joyce Farrell

Stanford University

450 Serra Mall, Stanford CA

{hblasins, joyce\_farrell}@stanford.edu

## Abstract

*Illumination plays an important role in the image capture process. Too little or too much energy in particular wavelengths can impact the scene appearance in a way that is difficult to manage by color constancy post processing methods. We use an adjustable multispectral flash to modify the spectral illumination of a scene. The flash is composed of a small number of narrowband lights, and the imaging system takes a sequence of images of the scene under each of those lights. Pixel data is used to estimate the spectral power distribution of the ambient light, and to adjust the flash spectrum either to match or to complement the ambient illuminant. The optimized flash spectrum can be used in subsequent captures, or a synthetic image can be computationally rendered from the available data. Under extreme illumination conditions images captured with the matching flash have no color cast, and the complementary flash produces more balanced colors. The proposed system also improves the quality of images captured in underwater environments.*

## 1. Introduction

Light is necessary for a camera to capture an image of a scene. Photons propagate from the light source, interact with objects and are focused by the lens onto sensor pixels. Images are often captured under different sources of illumination, as well as in photon-deprived conditions such as indoors, at night and in underwater environments.

There are two approaches to capturing images at low light levels. Passive strategies involve adjusting camera settings during the capture process. An increase in the sensor exposure time allows pixels to capture more photons, however any movement of the photographed target will produce blur in the image. Exposure durations can be decreased by increasing sensor gain (ISO) however this often increases the visibility of photon noise [26]. In both instances, varying exposure duration does not change the spectral power of the scene illumination.

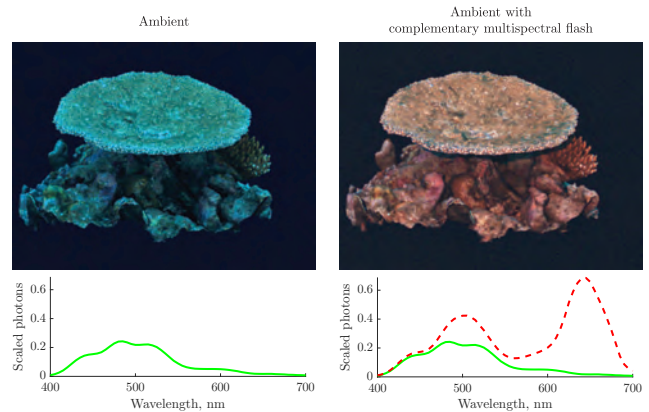


Figure 1. The red light component in daylight spectrum becomes absorbed when light travels underwater. This causes images captured underwater to have a strong greenish or blueish tint (left panels). A computational multispectral flash can estimate the ambient illuminant spectrum and adjust its own spectral power distribution (red dashed line) to provide the missing wavelength components and color balance the scene (right panels).

Active strategies include delivering more light into the scene with a light source controlled by the photographer. This approach dates back to the early days of photography, where additional light was delivered by igniting flash powder; a mixture of metallic fuel with oxidizer [24]. Over time powder was replaced by a Xenon light discharge and more recently high intensity light emitting diodes (LEDs).

Using an external light source solves the problem of photon scarcity, but very often produces unnaturally looking images with color tint [21]. This is due to a spectral power distribution mismatch between the low intensity ambient illumination and the light emitted by the flash. Such color artifacts are difficult to detect and correct during color balancing [9]. Some of these issues can be avoided when the temperature of the flash is adjusted to match the temperature of the ambient illumination, but this approach still requires a method to estimate the ambient spectrum.

In this work we describe a multispectral flash and the

accompanying computational algorithms. The flash is composed of a small number of individually controlled narrow-band lights. By adjusting their intensities the spectral power distribution of the light emitted by the flash can be modified. We describe how such a flash can be used to capture images of the scene in a way that makes it possible to estimate the spectrum of the ambient illuminant. Given this estimate we then propose to optimize the spectrum of the flash for two different imaging scenarios; *complementary* and *matching*.

The first scenario involves computation of the flash spectrum that would *complement* the light wavelengths missing from the ambient illuminant in order to produce a color balanced image. This use case is most applicable to situations where the ambient contains a lot of energy in some portions of the spectrum and very little in others. In addition to tungsten and fluorescent lighting conditions, we also consider the more extreme case of underwater imaging where water absorbs energy in the long wavelengths causing underwater photographs to have a strong green or blue tint (Figure 1). The methods we describe can also be applied to complement office fluorescent lighting and other ‘unbalanced’ lighting.

The other scenario involves adjusting the flash to *match* the illuminant spectrum in order to deliver more light into the scene. One can then either reduce exposure level to minimize blur or keep exposure level constant and minimize the visibility of photon noise.

In summary, our contributions include

- A new flash design for consumer applications with adjustable spectral power distribution of the light output,
- A method to estimate the ambient illuminant spectrum,
- New modes of flash spectrum adjustment: *complementary* that delivers light components missing from the ambient, and *matching* that reproduces the ambient light spectrum.

This paper is organized as follows; we briefly review related work in Section 2 and the image formation model in Section 3. We introduce the design of the multispectral flash, and the corresponding computational algorithms in Section 4. We evaluate the performance in a series of simulations in Section 5, and practical experiments in Section 6. The summary and conclusions are presented in Section 7.

## 2. Related work

The potential of flash, no-flash image pairs for computational photography applications has been extensively explored. Algorithms can be broadly categorized around image quality improvement, semantic analysis and surface property estimation.

One class of algorithms uses flash to improve image quality. For example, DiCarlo *et al.* presented a method

to estimate the ambient illuminant from a flash and no-flash image pair [5]. Eisemann and Durand combined color information from the no-flash image with the intensity of the flash image to create a detail rich image preserving the ambiance of the original scene [6]. These ideas were extended further by Petschnigg *et al.* who proposed a sequence of algorithms that used flash, no-flash image pairs to transfer image detail, enable white balancing and remove red-eye artifacts [18]. Zhuo *et al.* proposed a motion blurred image enhancement method, where the blur kernel was estimated from the flash, no-flash image pair [28]. Dark flash techniques use emitters outside of the visible range; in the ultra-violet and near-infrared, and leverage correlations between spectral channels to improve the quality of images captured in the visible portion of the spectrum [4, 12, 14].

Another class of methods uses flash to enhance semantic understanding of the scene. For example, Raskar *et al.* [20] extracted information about scene geometry from flash, no-flash images and performed image segmentation and stylized rendering. Sun *et al.* [21] captured images with and without a flash to robustly segment foreground from the background. Stereo flash, no-flash image pairs were also used to enhance depth estimation [27].

Multispectral light sources are primarily used for surface property estimation [2, 3, 16, 17]. These systems operate in the absence of ambient illumination and derive the reflectance and fluorescence properties from a sequence of images using inverse estimation methods.

Our work is most similar to that of Vasukscu *et al.* [22] who demonstrated that a spectrally tunable flash can improve color rendering in underwater environments. Unlike the authors, who fixed the spectrum of the flash for particular imaging conditions, we developed adaptable algorithms that can automatically adjust the flash spectrum to provide wavelengths that are missing from the ambient illumination. Also, unlike multispectral imaging systems that are designed to estimate surface reflectance, our system is easy to calibrate and only requires the knowledge of the spectral properties of the camera and light sources.

## 3. Image formation

The intensity  $m_j$  of a particular camera pixel is a linear function of the surface spectral reflectance  $r$ , the spectral responsivity of the  $j$ th camera channel  $c_j$ , and the total illumination  $i$

$$m_j = g \int r(\lambda) c_j(\lambda) i(\lambda) d\lambda. \quad (1)$$

The scalar  $g$  represents the gain and incorporates the effects of camera ISO setting, aperture diameter and the exposure duration.

The illumination  $i$  at every point in the scene can be decomposed into two components; global, ambient  $i_a$  that is

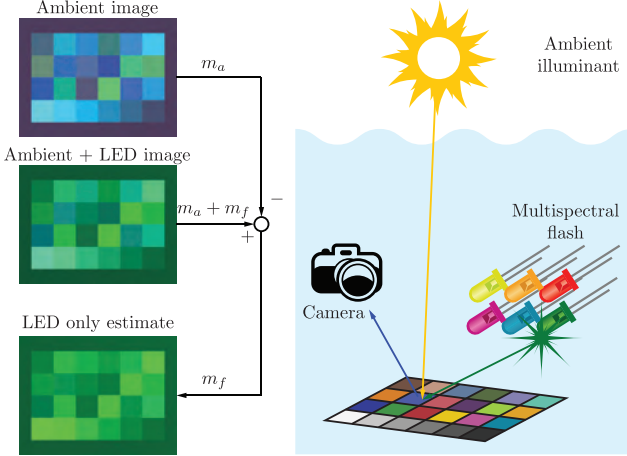


Figure 2. The imaging system equipped with a multispectral flash captures the image of the scene under the ambient illuminant, and a sequence with each of the narrowband lights turned on at a time. By linearity of image formation the flash only image can be estimated by subtraction.

beyond user's control, and the user controlled flash  $i_f$

$$i(\lambda) = i_a(\lambda) + i_f(\lambda). \quad (2)$$

For convenience, continuous wavelength variables can be discretized to  $n$  spectral bands, so that the image formation model becomes

$$\begin{aligned} m &= m_a + m_f \\ &= gC^T \text{diag}(r)i_a + gC^T \text{diag}(r)i_f, \end{aligned} \quad (3)$$

where  $C \in \mathbf{R}^{n \times n_c}$  is a matrix containing the spectral responsivities of the  $n_c$  camera channels (for consumer cameras  $n_c = 3$ ). Vectors  $r, i_a, i_f \in \mathbf{R}^n$  represent surface spectral reflectance, ambient and the flash illuminant spectra respectively. The  $\text{diag}(x)$  operator distributes the entries of  $x$  along the diagonal of a matrix.

#### 4. Multispectral flash

The multispectral flash we propose is an easy-to-build device that produces a small number  $k$  of spectrally narrowband lights. The intensity of each narrowband light is independently controlled, allowing us to shape the total emission spectrum of the flash. There are a variety of ways in which such a flash can be built. One way is to use bandpass filters together with broadband light sources, another way is to use high power LEDs.

The flash can be operated in a few different ways. For example, a flash, no-flash image pair can be captured and used with the illuminant estimation method of DiCarlo *et al.* [5]. In this case the flash is adjusted to produce a flat spectral

power distribution. This method however, requires a model for the spectral surface reflectance of imaged objects.

We propose a more flexible approach in which the acquisition system captures a sequence of images in quick succession. First we capture an image of the scene under the ambient illuminant only. Next, we collect a set of images where the scene is illuminated by a single narrowband as well as the ambient light. For a particular pixel this operation produces a sequence of measurements  $m_a, m_a + m_{f,1}, \dots, m_a + m_{f,k} \in \mathbf{R}^3$ . Due to linearity of image formation  $m_{f,k}$  are estimated by subtracting the measured pixel intensities of the ambient illuminant from the ambient and flash images (Figure 2). This image sequence is used to estimate the ambient illuminant spectrum and to compute the optimal spectrum of the flash operating in the *complementary* or *matching* modes.

#### 4.1. Illuminant spectrum estimation

The illuminant estimation is a fundamental problem in photography. In order to correctly render colors in captured images it is necessary to know the properties of the ambient illumination as the image is captured [25]. Most algorithms analyze pixel value statistics to estimate the spectrum of the illuminant [8], although active techniques have also been proposed [5].

The method we propose relies on finding a weighted sum of flash-only image intensities that best predicts the ambient image intensity. Unlike Legendre *et al.* [13], we perform spectral estimation rather than appearance matching, and we do not make any assumptions regarding surface spectral reflectances [5]. The weights applied to the flash-only image pixels that best approximate the ambient image can be found by solving a least-squares problem

$$\text{minimize} \left\| m_a - \sum_k w_{a,k} m_{f,k} \right\|, \quad (4)$$

where  $w_{a,k}$  represent the mixing weight scalars. Under the linear image formation model (3) this is equivalent to

$$\text{minimize} \left\| C^T \text{diag}(r) (i_a - Iw_a) \right\|, \quad (5)$$

where  $I \in \mathbf{R}^{n \times k}$  is a matrix whose columns contain the spectral power distributions of the narrowband lights under which the images were captured. Note that the above minimization can be interpreted as finding the best approximation to the ambient with the narrowband flashes *i.e.*  $i_a = Iw_a$ , up to a nullspace formed by camera sensor responsivities and surface spectral reflectance  $C^T \text{diag}(r)$ .

The optimization can be made more robust by incorporating prior knowledge about physical and statistical properties of natural illuminants. For example a modified opti-

mization problem

$$\begin{aligned} & \text{minimize} \left\| m_a - \sum_k w_{a,k} m_{f,k} \right\| + \alpha \left\| \nabla I w_a \right\| \\ & \text{subject to } I w_a \geq 0, \end{aligned} \quad (6)$$

enforces nonnegativity and imposes a roughness penalty on the estimated spectrum. The strength of the penalty is controlled by a scalar  $\alpha$  and  $\nabla$  is the 1<sup>st</sup> order difference operator.

Our illuminant estimation process is inherently self-calibrating. Unlike systems such as [2], the knowledge about the absolute intensity of the narrowband lights, nor the scalar gain  $g$  are not required. These unknown scale factors are incorporated directly into the estimated weights  $w_a$ . This robustness makes practical implementations easier.

#### 4.2. Flash spectrum adjustment

The information about the spectral power distribution of the ambient illuminant can be used to adjust the spectrum of the flash. We propose two different strategies for adjusting the flash spectrum. One approach is to *match* the flash and the ambient illuminant spectra so that the relative spectral power distribution of the ambient and the light delivered by the flash are similar. The other is to adjust the flash to *complement* the ambient illuminant. In this mode, the flash delivers light at wavelengths missing from the ambient illumination.

Once the ambient illuminant spectrum is known the *matching* flash can be easily derived by solving a least-squares problem

$$\begin{aligned} & \text{minimize} \left\| C^T I(w_a - w_f) \right\| \\ & \text{subject to } 1 \geq w_f \geq 0, \end{aligned} \quad (7)$$

where  $I w_a$  is the estimated ambient illuminant spectrum and  $w_f \in \mathbf{R}^{n_f}$  is a vector containing the *matching* flash intensity weights. To achieve the best performance, and to deliver the largest amount of light into the scene the estimated flash weights can be scaled so that  $\max(w_f) = 1$ . This operation will not change the shape of the flash spectrum but maximize its intensity.

The *complementary* flash is particularly useful under extreme illumination conditions where the ambient light contains little energy in some portions of the spectrum, and a lot in others. Many color balancing algorithms use a von Kries like transformation to adjust the gains of the red, green and blue camera channels [8, 23]. When a particular channel carries little energy, the corresponding gain is large. Unfortunately, in noise limited systems this process accentuates the noise component leading to poor visual effects (Figure 3). In those cases the spectrally adjustable flash in



(a) Raw image

(b) Color balanced

Figure 3. Conventional, von Kries like color balancing algorithms amplify the noise when applied for underwater image correction where little light is present in the red camera channel (best viewed on a computer screen).

the *complementary* mode will deliver photons at the precise wavelengths missing from the ambient illumination.

Consider the estimated spectrum of ambient illuminant to be  $I w_a \in \mathbf{R}^n$ . The goal is to find such spectral power distribution of the flash that complements this ambient to some desired illuminant spectrum  $i_d \in \mathbf{R}^n$ . The optimal flash weight assignment  $w_f \in \mathbf{R}^{n_f}$  that will *complement* the desired illuminant spectrum is given by

$$\begin{aligned} & \text{minimize} \left\| C^T I(w_a + w_f) - s C^T i_d \right\| \\ & \text{subject to } 1 \geq w_f \geq 0, \end{aligned} \quad (8)$$

$$s \geq 0. \quad (9)$$

The scalar  $s$  is a slack variable that makes the system intensity scale invariant. The inequality constraint (8) applies bounds on the intensity of each of the narrowband lights from the multispectral flash. When  $w_f = 1$  then the light is fully on and emits maximal amount of light, when  $w = 0$  it is off, with intermediate states in between.

#### 4.3. Image capture

To capture dynamic scenes with fast moving objects the final image can be acquired during a single exposure, with the flash producing light of the desired spectrum. The constraint (8) assures that the flash spectrum is physically realizable, can be produced by hardware and delivered into the scene.

An alternative to re-capturing images with a correctly adjusted flash spectrum is to take advantage of the linearity of image formation model. An equivalent image can be synthesized by computing a sum of the ambient image  $m_a$  and led only images  $m_f$  weighted by the corresponding flash weights (Figure 4). When operating in the computational flash mode, the constraint (8) is no longer required, and may be dropped from the optimization.

This computational approach has two disadvantages. First, for dynamic scenes, objects could have moved in the time between the first and last frames were captured producing a blurry image. Second, if the constraint (8) is ig-

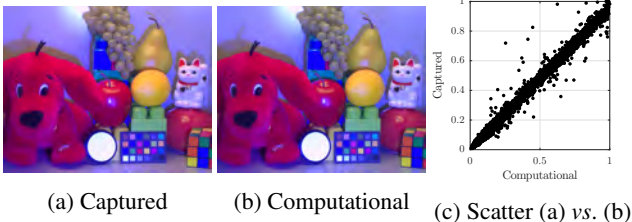


Figure 4. Computational image synthesis is equivalent to re-capturing the image of the scene under the computed flash spectrum due to the linearity of the image formation model.

Table 1. Quantitative root-mean-squared error (RMSE) for different number of narrowband lights forming the multispectral flash. All error metrics decrease as the number of lights increases. The accuracy of spectrum estimation approaches that of a multispectral system for six LEDs.

# LEDs	3	4	5	6	7
Pixel ( $\times 10^{-2}$ )	1.5	1.0	0.4	0.3	0.2
CIE $xy$ ( $\times 10^{-2}$ )	0.3	0.1	0.05	0.03	0.03
Spectrum	0.22	0.18	0.16	0.13	0.13
Multispectral	0.14	0.12	0.14	0.13	0.13

nored, some of the entries of  $w_f$  can become large, amplifying noise in the final image.

## 5. Simulations

We evaluated the performance of the proposed illuminant estimation algorithm using the ISET camera simulation software package [7]<sup>1</sup>. In our simulations, we created a test chart composed of 110 different surfaces with natural spectral reflectance properties. The chart was illuminated with lights having different chromaticity coordinates in the CIE  $xy$  space. We varied, between three and seven, the number of narrowband LEDs which formed the multispectral flash. We also evaluated the influence of camera spectral properties on the accuracy of the estimated illuminant spectrum. We examined 34 different camera models we calibrated ourselves or used the spectral responsivity functions from [11].

The quality of the ambient illuminant estimate depends on the distribution and variability of surface spectral reflectances present in the scene. We explore this relationship by providing the illuminant estimation algorithm with simulated pixel intensities from different numbers of patches from the test chart. We randomly draw, with repetition, a fixed number of patches from our 110-patch chart and use this set to estimate the illuminant spectrum. The sampling

<sup>1</sup>Code available for download at <https://github.com/hblasins/compMultispFlash.git>

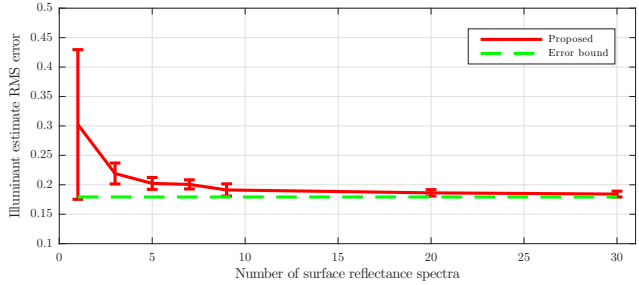


Figure 5. Errors in the illuminant spectrum estimate decrease with increasing variability in scene surface spectral reflectances. When about 10 different surfaces are visible, the error approaches the lower bound set by directly approximating the illuminant spectrum with a given number of LED spectra.

process is repeated 10 times for each patch collection size we evaluate. In this simulation we fix the illuminant chromaticity coordinates ( $x = 0.2, y = 0.2$ ) the camera spectral responsivities and we use a multispectral flash with seven LEDs. For each illuminant spectrum estimate we compute the RMS error with the ground truth. Figure 5 demonstrates that the errors plateau when a scene contains about 10 distinct reflectance spectra.

Pixel RGB values of a surface illuminated with an ambient illuminant can be approximated with RGB values of the same surface illuminated with narrowband lights, as long as the RGB pixel values of the ambient are within the convex hull formed by the RGB values of the narrowband lights. Our simulations show that this is only approximately true when three or four narrowband lights are used. The root-mean-squared errors (RMSE) values, both for pixel as well as spectral power distributions, (Table 1) are high. Furthermore, for those cases we observed large variability across different camera models.

Figure 6 compares the estimated and measured ambient illuminant spectra for different numbers of LEDs. The estimates improve and become camera invariant when at least five LEDs are used. With six or more LEDs in use the errors in illuminant spectrum estimates asymptote and approach the error achieved by direct optimization of LED weights in the wavelength domain, *i.e.*  $\min \|i_a - Iw_a\|$ . A multispectral flash with seven LEDs can accurately reproduce the ambient illuminant spectrum across many different illuminant chromaticities (Figure 7). Also note that linear models for the reflectance of objects typically require 6–7 spectral basis functions [10].

## 6. Experiments

We also conducted experiments using real scenes, illuminants and narrowband lights. We assembled a collec-

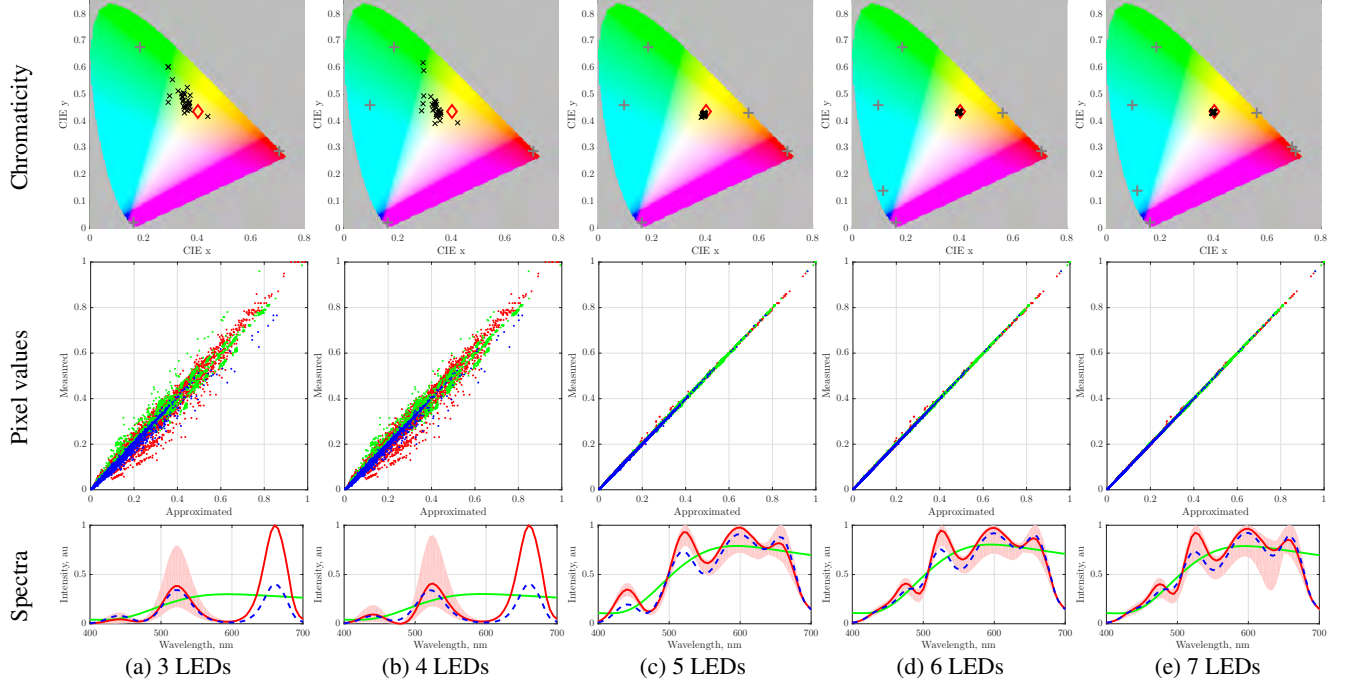


Figure 6. Spectral estimation accuracy increases with the number of narrowband illuminants in the spectral flash. Even when the chromaticity of the illuminant (◇) falls within the convex hull of the LED chromaticities (+), at least five LEDs are needed to approximate camera pixel intensities. Black  $\times$  represent variability in chromaticity coordinates of the estimated illuminant across different camera models. This variability is also represented by red shaded areas in the *Spectra* plots, where the red solid line shows the average spectrum estimate. These plots also contain the ground truth spectrum (—) and the best least-squared approximation under the narrowband illuminants (—).

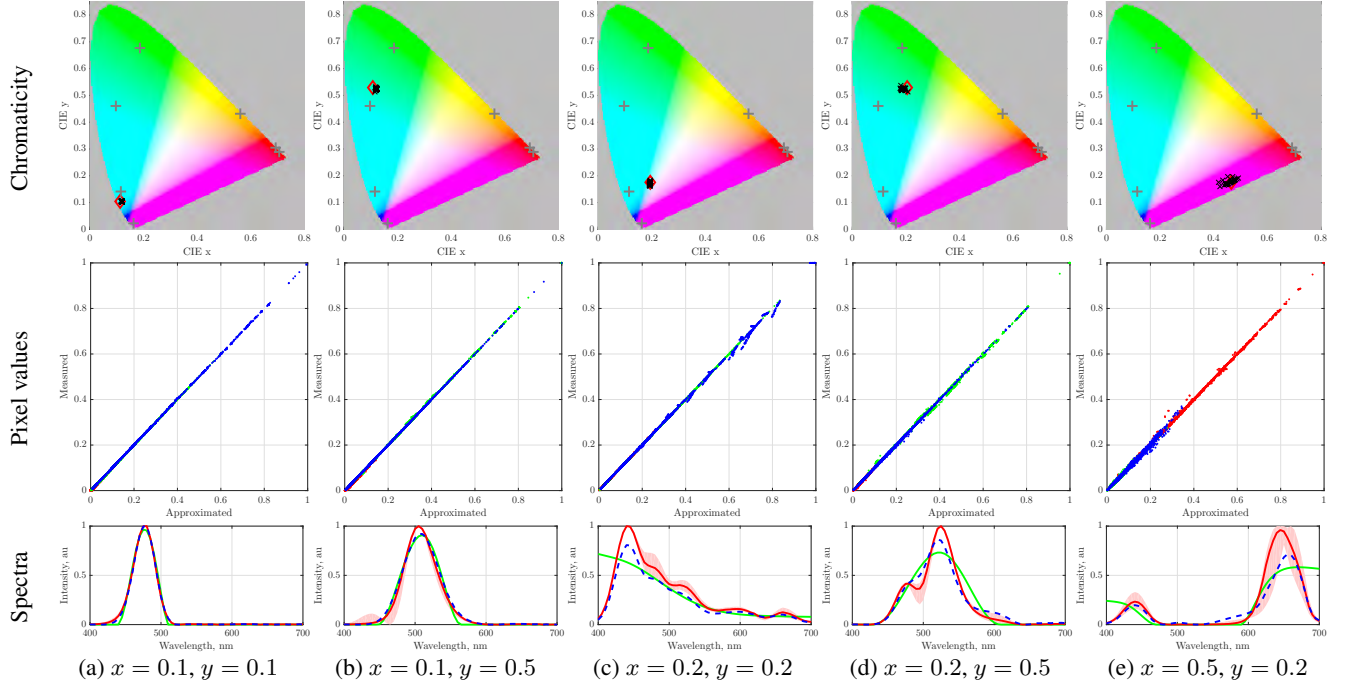


Figure 7. Estimation accuracy is independent of the illuminant spectrum, and the spectral properties of the camera provided that the multispectral flash contains sufficiently many narrowband illuminants. Different columns correspond to lights with different CIE  $xy$  chromaticity coordinates, that are approximated with seven narrowband lights. Refer to Figure 6 for notation details.

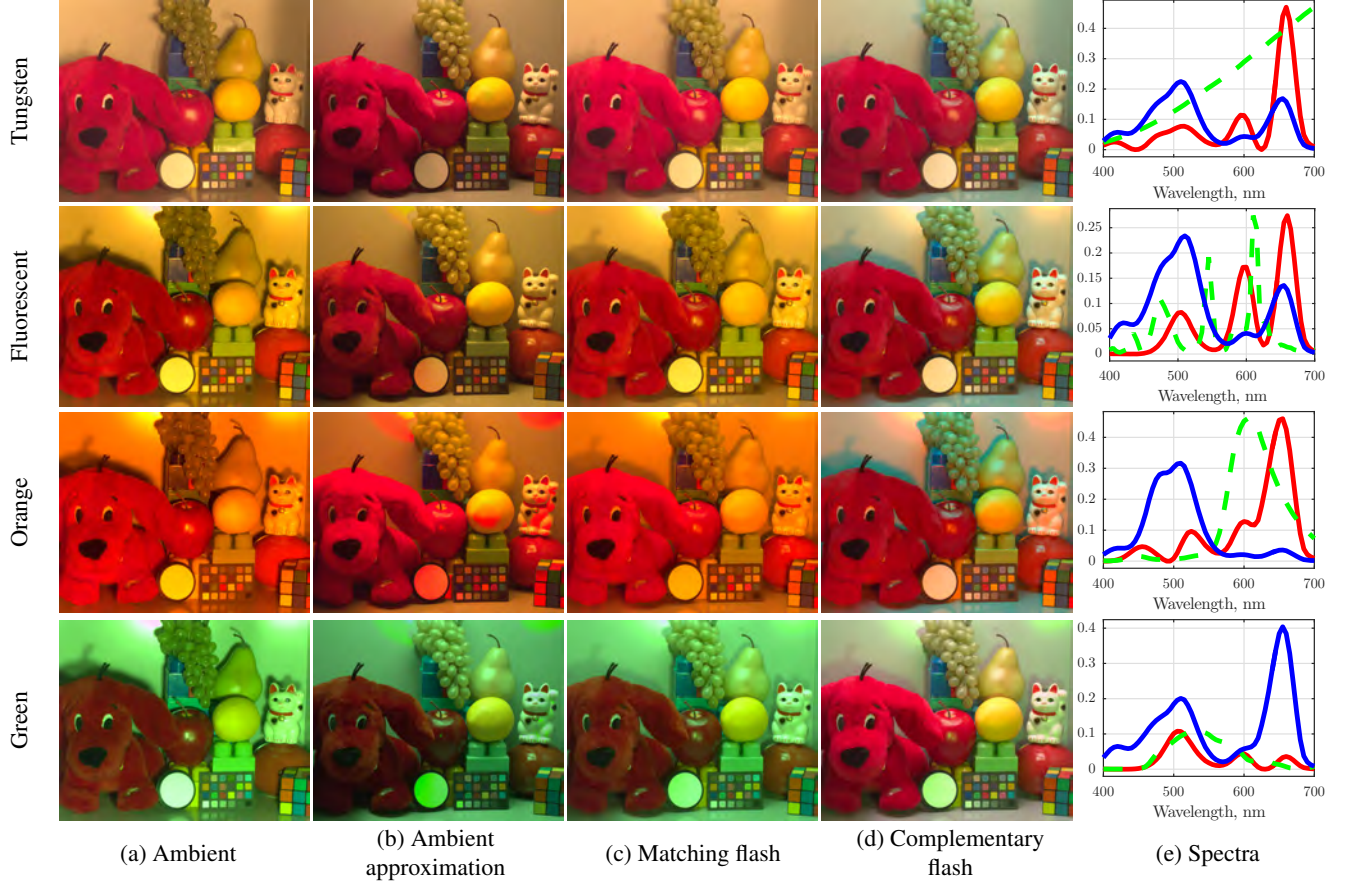


Figure 8. Computational spectral flash can adjust its spectral power distribution to deliver light that is similar (*matching mode*) or that delivers the wavelengths that are missing (*complementary mode*) from the ambient. Each row represents a different ambient illumination condition. Columns represent the ambient image (a), its linear approximation with narrowband light images (b) and images captured with the computational flash in the *matching* (c) and *complementary* (d) modes. Curves in (e) show the illuminant spectral power distributions of the ambient (green, dashed), estimated ambient (red) and the ambient complement (blue).

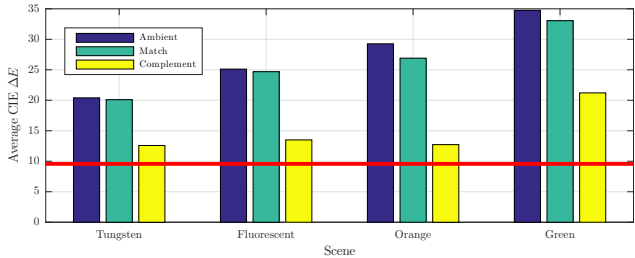


Figure 9. Average Macbeth chart CIE  $\Delta E$  errors. Appearance comparison between the chart imaged under the D65 illuminant and the chart illuminated with different ambient lights and the multispectral flash. The complementary flash mode reduces color rendering errors. Red line represents the lowest error that can be achieved when approximating D65 with LEDCube narrowband lights.

tion of natural objects inside a LEDCube light booth<sup>2</sup>. The booth contains eight different narrowband LEDs which we adjusted to model the spectral flash. The interior of the booth was illuminated from the outside with different narrowband and broadband light sources. Finally, we captured images with a 1.3 megapixel Ximea xiQ (MQ013CG-E2) RGB camera.

Figure 8 shows the test scene captured under a variety of ambient illuminants. Images were minimally processed for rendering purposes; corrected for different sensitivities of color channels and gamma encoded. These processing steps were identical across all conditions. We estimated the spectrum of the ambient light using all non-saturated pixels and assumed that the light was spectrally uniform across the entire scene. Even this very simplistic assumption proved to work well in the conditions we tested. First we estimated the ambient illumination spectrum by approximating the

<sup>2</sup><http://www.thouslite.com/show.asp?id=16>

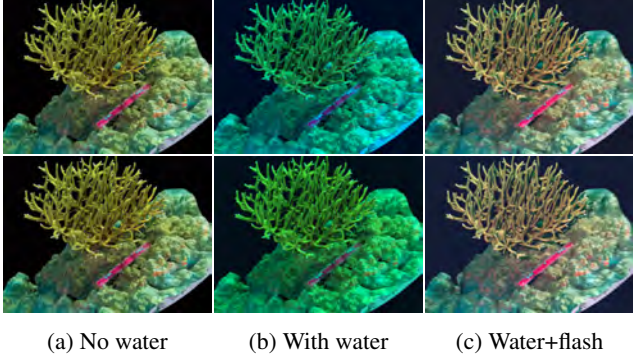


Figure 10. Underwater scene simulation. The original colors in the scene (a) are distorted in the presence of different water types (b), but are recovered when the multispectral flash in the *complementary* mode is used (c).

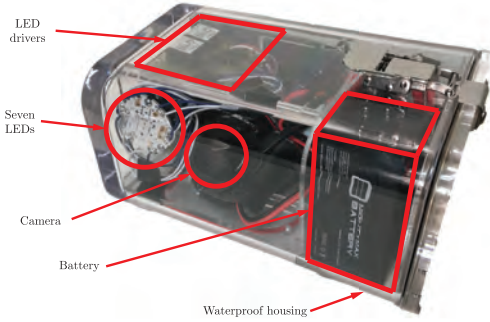


Figure 11. The portable, ruggedized version of the computational spectral flash built for underwater photography applications. Camera and LEDs are synchronized using a Raspberry Pi mini-computer (not shown).

ambient image with a weighted sum of the narrowband only images (Figure 8a, 8b). Given the illumination spectrum we then rendered scene images under matching (Figure 8c) and complementary flash spectra (Figure 8d). Note that the estimated illuminant spectra (Figure 8e, red line) are imperfect, but correctly identify the bands, where the ambient light delivers the most energy. This is sufficient to produce images without color cast due to the flash in the *matching* mode, or with more balanced colors under the *complementary* flash.

To demonstrate the improvement in color rendering we computed CIE  $\Delta E$  error metrics between an image of a Macbeth chart captured under a standard D65 illuminant and images captured with our computational flash. In our measurements we assumed that images were displayed on an sRGB color monitor, with D65 as the white point. Figure 9 demonstrates that the matching flash does not affect the colors, while the complementary flash reduces color reproduction errors.

The final image appearance is also affected by the directionality of light and scene geometry. The computational

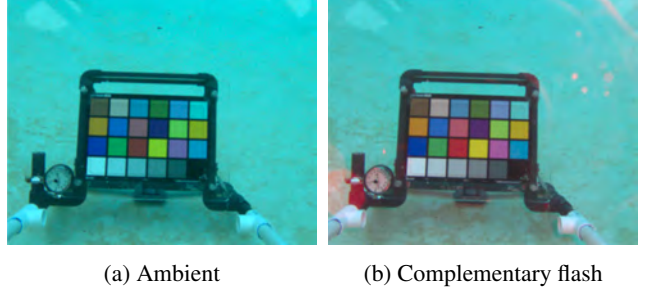


Figure 12. Underwater photography with computational multispectral flash. The flash operating in the *complementary* mode can deliver the red light that is missing from the ambient underwater conditions.

spectral flash will adapt to the ambient light spectral power distribution, but will physically be located at a different point in space. For this reason the *matching* and *complementary* flash images are, in general, unable to reproduce the same shading effects as in the original image.

## 6.1. Underwater imaging

Imaging in water is more difficult because light interacts with the volume of water through absorption and scattering phenomena. For clear waters, the effects of scattering are small, and absorption is the primary factor influencing image appearance. Absorption is a wavelength dependent process that reduces the intensity of light traveling in a certain direction and depends on the distance through medium that the light covers. When the camera is close to the target, relative to the depth, light is primarily affected by the water column between the target and the surface. Under this simplistic model, underwater scenes are illuminated by a significantly distorted daylight spectrum, which typically has little energy in the long wavelengths ( $>\sim 600\text{nm}$ ).

The specific spectral shape of the underwater ambient depends not only on the depth but also the chemical composition of water and, in general, varies a lot. Figure 10 shows renderings of coral reef models above and underwater, and demonstrates the effects of water composition variability on image appearance. These images were generated using PBRT ray-tracing software [19] and a water model of [1, 15]. We also used the same rendering environment to simulate the images a camera with a computational multispectral flash would capture and how the *complementary* flash algorithm helps recover the original scene colors. The proposed *complementary* flash algorithm makes it possible to recover much of the scene appearance lost due to water absorption.

To evaluate the performance of the proposed system in real underwater photography applications we built an underwater version of the computational multispectral flash. The system was battery powered and used the same Ximea

xiQ color camera, seven Luxeon Star high power LEDs with BuckPuck led drivers, and a Raspberry Pi 3 computer for data capture and synchronization. The system was enclosed by a waterproof Ikelite 5710 Housing (Figure 11).

Figure 12 shows an image of a Macbeth chart captured in a swimming pool a depth of about 5 meters with and without the *complementary* flash. Even though at this depth the light still contains some energy in the red portion of the spectrum, its intensity is reduced. The *complementary*, computational multispectral flash algorithm can correctly estimate that the red component is attenuated and can adjust the flash spectrum accordingly making colors more vivid and natural.

## 7. Conclusions

We presented a computational multispectral flash composed of a small number of narrowband lights. We showed how to use this device to derive the ambient illuminant spectrum. Given the ambient estimate, we programmed the flash to produce two types of light spectra. In the *matching* mode, the spectrum produced by the flash is visually similar to the ambient and consequently does not change the color cast. In the *complementary* mode the flash delivers the light at wavelengths that are missing from the ambient illumination and produces more natural-looking images. We also showed that the desired effects can be achieved computationally from the acquired set of images.

The color balancing effect of the *complementary* flash becomes useful in environments where certain wavelengths are missing from the ambient illumination. For example light underwater typically does not contain any energy in the longer wavelengths ( $>\sim 600\text{nm}$ ). Consequently red is absent from underwater images. We showed, through simulations and experiments that the computational multispectral flash enhances underwater image quality.

The design and the algorithms have some limitations. The flash is physically located at a particular spatial location and therefore it cannot reproduce the same shadow effects as the ambient light. The algorithms we presented operate under the simplifying assumption that the light spectrum is uniform across the scene. In the future we plan on exploring patch based methods where the ambient and the flash spectra are estimated locally thus allowing for spectral variability across the whole scene.

## Acknowledgements

The authors would like to thank Brian Wandell from Stanford University for helpful discussions and comments and Erika Woosley from The Hydrous for providing meshes and textures of different 3D coral models.

## References

- [1] H. Blasinski and J. Farrell. A three parameter underwater image formation model. *Electronic Imaging*, 2016(18):1–8, 2016.
- [2] H. Blasinski, J. Farrell, and B. Wandell. An iterative algorithm for spectral estimation with spatial smoothing. In *IEEE International Conference on Image Processing, ICIP*, pages 936–940, Sept 2015.
- [3] H. Blasinski, J. Farrell, and B. Wandell. Simultaneous surface reflectance and fluorescence spectra estimation. *arXiv preprint arXiv:1605.04243*, 2016.
- [4] B. Choi, Y. Ha, and D. Kim. Multi-spectral flash imaging using weight map. *Proceedings of the 19th Korea-Japan Joint Workshop on Frontiers of Computer Vision, FCV*, pages 272–275, 2013.
- [5] J. DiCarlo, F. Xiao, and B. Wandell. Illuminating illumination. In *Color and Imaging Conference*, pages 27–34. Society for Imaging Science and Technology, 2001.
- [6] E. Eisemann and F. Durand. Flash photography enhancement via intrinsic relighting. *ACM Transactions on Graphics*, 23(212):673, 2004.
- [7] J. Farrell, F. Xiao, P. Catrysse, and B. Wandell. A simulation tool for evaluating digital camera image quality. In *Electronic Imaging 2004*, pages 124–131. International Society for Optics and Photonics, 2003.
- [8] A. Gijsenij, T. Gevers, and J. van de Weijer. Computational color constancy: Survey and experiments. *IEEE Transactions on Image Processing*, 20(9):2475–2489, Sept 2011.
- [9] E. Hsu, T. Mertens, S. Paris, S. Avidan, and F. Durand. Light mixture estimation for spatially varying white balance. In *ACM Transactions on Graphics (TOG)*, volume 27, page 70. ACM, 2008.
- [10] T. Jaaskelainen, J. Parkkinen, and S. Toyooka. Vector-subspace model for color representation. *J. Opt. Soc. Am. A*, 7(4):725–730, Apr 1990.
- [11] J. Jiang, D. Liu, J. Gu, and S. Susstrunk. What is the space of spectral sensitivity functions for digital color cameras? In *IEEE Workshop on Applications of Computer Vision, WACV*, pages 168–179, 2013.
- [12] D. Krishnan and R. Fergus. Dark flash photography. *ACM Transactions on Graphics*, 28(3):1, 2009.
- [13] C. LeGendre, X. Yu, D. Liu, J. Busch, A. Jones, S. Pattanaik, and P.Debevec. Practical multispectral lighting reproduction. *ACM Transactions on Graphics*, 35(4):32, 2016.
- [14] S. Matsui, T. Okabe, M. Shimano, and Y. Sato. Image enhancement of low-light scenes with near-infrared flash images. *Lecture Notes in Computer Science*, pages 213–223, 2010.
- [15] C. Mobley. *Light and water: Radiative transfer in natural waters*. Academic Press, 1994.
- [16] J. Park, M. Lee, M. Grossberg, and S. Nayar. Multispectral imaging using multiplexed illumination. In *IEEE International Conference on Computer Vision, ICCV*, pages 1–8, Oct 2007.
- [17] M. Parmar, S. Lancel, and J. Farrell. An LED-based lighting system for acquiring multispectral scenes. In *Proc. SPIE*, volume 8299, pages 82990P–82990P–8, 2012.

- [18] G. Petschnigg, R. Szeliski, M. Agrawala, M. Cohen, H. Hoppe, and K. Toyama. Digital photography with flash and no-flash image pairs. *ACM Transactions on Graphics*, 23(3):664, 2004.
- [19] M. Pharr and G. Humphreys. *Physically based rendering: From theory to implementation*. Morgan Kaufmann, 2004.
- [20] R. Raskar, K.-h. Tan, R. Feris, J. Yu, and M. Turk. Non-photorealistic Camera : Depth Edge Detection and Stylized Rendering using Multi-Flash Imaging. *ACM Transactions on Graphics*, 23(3):679–688, 2006.
- [21] J. Sun, S. Kang, Z. Xu, X. Tang, and H. Shum. Flash cut: Foreground extraction with flash and no-flash image pairs. In *IEEE Conference on Computer Vision and Pattern Recognition, CVPR*, pages 1–8, 2007.
- [22] I. Vasilescu, C. Detweiler, and D. Rus. Color-accurate underwater imaging using perceptual adaptive illumination. *Autonomous Robots*, 31(2-3):285–296, 2011.
- [23] J. von Kries. Die gesichtsempfindungen. *Handbuch der physiologie des menschen*, 3:109–282, 1905.
- [24] D. Wood. The importance of artificial light in the development of night photography. In *Annual Meeting of the Association for Education in Journalism*, 1975.
- [25] F. Xiao, J. Farrell, J. DiCarlo, and B. Wandell. Preferred color spaces for white balancing. In *Proc. SPIE*, volume 5017, pages 342–350, 2003.
- [26] F. Xiao, J. Farrell, and B. Wandell. Psychophysical thresholds and digital camera sensitivity: the thousand-photon limit. In *Electronic Imaging*, pages 75–84. International Society for Optics and Photonics, 2005.
- [27] C. Zhou, A. Troccoli, and K. Pulli. Robust stereo with flash and no-flash image pairs. In *IEEE Conference on Computer Vision and Pattern Recognition, CVPR*, pages 342–349, 2012.
- [28] S. Zhuo, D. Guo, and T. Sim. Robust flash deblurring. In *IEEE Conference on Computer Vision and Pattern Recognition, CVPR*, pages 2440–2447, 2010.